Thermoelastic Analysis of Space Structures in Periodic Motion

Dan Givoli* and Omri Rand*
Technion—Israel Institute of Technology, Haifa, Israel

Large truss-type space structures undergoing periodic motion are analyzed using Fourier decomposition in time and finite elements in space. Both the temperature field and the displacement field in the structure are found. Any symmetry which the structure may possess with respect to the axis of rotation is exploited in the numerical scheme and leads to saving in computational cost. A general algorithm is devised to calculate the external heat flux distribution. Numerical examples, which include a rotating cylindrically shaped structure and a parabolic antenna dish in orbit around Earth, are presented. The transition between the quasisteady state and the dynamic state in both the thermal and the elastic analyses is discussed in view of the numerical results.

Nomenclature

A = cross-sectional area
c = specific heat
E = Young's modulus
F = the load vector
G = the capacity matrix
k = thermal conductivity
K = the stiffness matrix
M = the mass matrix
p = perimeter of the member's cross section
P = the conductivity matrix
q = a given time-periodic incident flux
Q = the thermal load vector
R = the radiation vector
s = axial coordinate along the rod
t = time
T = temperature vector
$T(s,t)$ = temperature
T_{ref} = a reference temperature in which the truss is undeformed
$u(s,t)$ = axial displacement
α = coefficient of thermal expansion
ϵ = surface emissivity of the truss member
ρ = mass density
σ = the universal Stefan-Boltzmann constant

Introduction

THE thermal and structural design and analysis of large space structures have caught much attention in the last few years. Space structures are typically three-dimensional truss-type structures, which are exposed to thermal loading in the form of solar radiation, infrared planetary radiation and planetary albedo (solar radiation reflected from planets). Finding the spatial and temporal variation of the temperature field in the structure resulting from this radiation is important for the thermal design. In addition, the dynamic temperature field may also give rise to the dynamic deformation of the structure. This deformation is of interest due to the limitations on the allowed magnitude of the deflection of instruments and antennas and due to the necessity to avoid a resonance.

Received April 25, 1990; revision received Sept. 9, 1990; accepted for publication Sept. 19, 1990.
*Assistant Professor, Department of Aerospace Engineering.

Works that have dealt with this subject may be divided roughly into two categories: those that are concerned with general concepts and preliminary design issues and those that involve an accurate analysis of a specific type of models. The former type of works include Refs. 1-10. Foldes and Dienemann[1] and Archer[2] discuss the performance requirements for large multibeam antenna systems and the considerations involved in the design of the reflectors used with these systems. Based on these considerations, Clark and Allen[3] describe the evolution of the Hughes HS 376 reflector thermal design. Mikulas et al.[4] describe some design concepts for the space station truss structure and consider several approaches regarding the construction of the structure in space. Nash and Lardner[5] discuss the relative importance of the various factors influencing the mechanical response of large space structures. The authors consider both truss structures and thin membranes. Anderson and Nimmo[6] propose to use statically determinate trusses for large platforms and to compare the frequencies of such trusses with those of redundant ones. Ard[7] and Hedgepeth and Miller[8] discuss structural concepts of large parabolic antenna reflectors or solar concentrators and especially design concepts for deployable reflectors. Peskett and Gethin[9] consider various aspects of the thermal design and analysis of a spacecraft, including the derivation of the thermal loading. They also perform a case study analysis of an orbiting structure. Ory et al.[10] consider in detail some preliminary design aspects for large orbiting platforms and propose two alternative structural configurations.

References 11-16 belong to the second type of works, which involve accurate computer analysis. Thornton et al.[11] describe an integrated thermal-structural finite element formulation with solar radiation and use a three member module of an orbiting truss as a testing model. Thornton and Paul[12] review the subject of computerized thermal-structural analysis of large space structures and use for illustration a tetrahedral truss structure as a model for a microwave radiometer system. Mahaney and Thornton[13] investigate the effects of self-shadowing on the thermal-structural behavior of space structures. Their numerical experiments indicate that such effects are significant and must be included in the calculations. Ko[14] describes in detail the thermal and elastic analyses performed for the Space Shuttle Orbiter, including internal convection and radiation effects. Thermal stresses are found to be very sensitive to variation in temperature distribution.

Lutz et al.[15] propose to use different finite element models for the thermal and structural analyses of a frame-type structure. The temperature field is first determined at selected cross sections of some of the beam members, via a two-dimensional finite element analysis. The forces and moments due to this temperature distribution are then calculated, and the global

structural response of the structure is obtained from the finite element model of the three-dimensional frame. Rand and Givoli[16] propose a numerical method for thermal and elastic problems with periodic loading, which combines finite element spatial decomposition and spectral treatment in time. The method is proposed as a basis for the analysis of large space structures, although an actual space structure model was not considered.

In this paper, the method developed in Rand and Givoli[16] is extended in two directions. The first extension has to do with the exploitation of geometrical symmetry, and the second extension is in the development of a general algorithm for computing "view factors." Then, the generalized scheme is applied to large space structures that are either rotating or orbiting. In the next section, the numerical method is summarized, and it is shown how one can exploit an existing symmetry of the structure with respect to the axis of rotation. Taking advantage of such symmetry may reduce the computational effort considerably. A general algorithm for the calculation of the view factors of all of the structural members (or the external heat flux distribution) is presented next. This algorithm makes a distinction between "transparent" and "opaque" structures or parts of structures. In the section that follows, the method is applied to a cylindrically shaped truss structure that spins around its axis and to a parabolic antenna dish mounted on a spacecraft which orbits around Earth. The numerical results indicate the existence of a critical angular velocity above which a quasisteady state assumption cannot be valid. A simplified model, which yields an analytic estimate of this critical angular velocity for both the thermal and elastic analyses, is proposed.

Numerical Method and Exploitation of Symmetry

Consider a three-dimensional truss structure exposed to a time-periodic incoming heat flux, with a period of $2\pi/\omega$. This periodicity may originate, for example, from the fact that the structure orbits around the Earth or that the structure rotates around a certain axis. Each truss member emits radiation to space. The incident heat flux gives rise to a time-dependent temperature field, which in turn induces the dynamic deformation of the structure. The analysis that follows is based on the following simplifying assumptions:

1) The members are assumed to be slender, so that variation of temperature within the cross section may be neglected.

2) The joints are considered perfect conductors and lacking any heat capacity.

3) The usually weak effect of heat exchange through radiation between different truss members is neglected.

4) The radiation emitted from the two ends of each member and the incident heat flux on these edges are neglected.

5) The coupling between the temperatures and the strains is neglected. More precisely, the strain rate and displacement fields are assumed not to affect the temperature field.

6) It is assumed that the truss members can only sustain axial forces and that the flexibility and mass of the joints can be neglected.

7) Structural energy dissipation (damping) is neglected.

8) While self-shadowing effects are taken into account for a structure covered with an opaque material, the effect of self-shadowing of the truss members themselves for a transparent structure is neglected.

In each truss member, the temperature field is governed by the nonlinear equation

$$\rho c \frac{\partial T}{\partial t} = \frac{\partial}{\partial s}\left(k \frac{\partial T}{\partial s}\right) - C_R T^4 + q \tag{1}$$

whereas the displacement field is governed by the linear equation

$$\rho A \frac{\partial^2 u}{\partial t^2} = \frac{\partial}{\partial s}\left[EA\left(\frac{\partial u}{\partial s} - \alpha(T - T_{\text{ref}})\right)\right] \tag{2}$$

In Eq. (1), C_R is the radiation coefficient given by

$$C_R = \sigma \epsilon \frac{p}{A} \tag{3}$$

In the case where the structure spins, the axial component of the centrifugal force $\rho A \omega^2 r$ (where r is the distance from the axis of spin) is added to the right-hand side of Eq. (2).

The consistent finite element discretization of Eqs. (1) and (2) leads to the two following systems of ordinary differential equations in time:

Thermal:

$$G\dot{T}(t) + PT(t) + R[T(t)] = Q(t) \tag{4}$$

Elastic:

$$M\ddot{d}(t) + Kd(t) = F(t) \tag{5}$$

In Eq. (4) the vector T contains the unknown temperatures at the nodes, and the vector R depends nonlinearly on it. In Eq. (5) d contains the unknown displacements at the nodes in the directions x, y, and z. A dot indicates differentiation with respect to time. In both Eqs. (4) and (5), periodic solutions with period $2\pi/\omega$ are sought.

The system of Eq. (4) has to be solved first for the temperature vector $T(t)$. Then $T(t)$ is substituted in the right-hand side of Eq. (5), which is solved to yield the displacement vector $d(t)$. The number of equations in Eqs. (4) and (5) depend on the finite element models chosen for the thermal and elastic problems and on the number and type of boundary conditions imposed. For later reference, let M_T and M_d be the number of equations in Eqs. (4) and (5), respectively.

The method of solution of Eqs. (4) and (5) is based on the discrete Fourier decomposition of each time-dependent function in Eqs. (4) and (5) into a finite number of harmonics N. In other words, if $f(t)$ is any vector variable appearing in Eqs. (4) and (5), then it is approximately represented by the finite Fourier expansion

$$f(t) \simeq f_0 + \sum_{n=1}^{N} (f_{cn} \cos n\psi + f_{sn} \sin n\psi) \tag{6}$$

Here f_0, f_{cn}, and f_{sn} ($n = 1, \ldots, N$) are real constant vectors, and ψ is nondimensional time or azimuth angle $\psi = \omega t$. Expressions such as Eq. (6) are used for all of the variables in Eqs. (4) and (5). The coefficients Q_0, Q_{cn}, and Q_{sn} as well as F_0, F_{cn}, and F_{sn}, associated with the thermal and elastic loads vectors Q and F, are found using a fast Fourier transform (FFT) scheme. Then, from Eqs. (4) and (5), one obtains a system of algebraic equations for the unknown coefficient vectors T_0, T_{cn}, T_{sn}, d_0, d_{cn}, and d_{sn}. All of the calculations involving arithmetic manipulation of the Fourier series representations of Eq. (6) are performed *symbolically* by the computer code itself, in the manner explained in Rand and Givoli[16] and Rand.[17] Equation (4) yields a nonlinear algebraic system of $M_T(2N + 1)$ equations and unknowns, which is solved via a Newton-Raphson type iterative procedure, whereas Eq. (5) yields a linear algebraic system of $M_d(2N + 1)$ equations and unknowns, which is solved by standard Gauss elimination.

The comparison of this method to the standard time-integration of Eqs. (4) and (5) using finite differences in time is discussed in detail in Rand and Givoli.[16] The proposed method is shown to be superior in many cases. Another advantage that the present method has is the ability to incorporate and exploit structural symmetry in a very simple and natural manner, as shown next.

Concentrating first on the thermal analysis, we note that many geometrical configurations of space structures possess a certain kind of symmetry, which will be defined as follows. Suppose that the total set of finite element nodes may be divided into a number of subsets, each subset having what

may be termed "delayed equivalence" among its members. This means that any two nodes i and j belonging to the same subset have the same temperature with a constant time delay between them. In other words, if $T_i(t)$ and $T_j(t)$ are the temperatures of nodes i and j, respectively, then $T_i(t) = T_j(t-\tau_{ij})$, where τ_{ij} is a constant time delay depending on i and j. In terms of the azimuth angle ψ, there is a constant phase shift between the two nodes: $T_i(\psi) = T_j(\psi - \Delta\psi_{ij})$, where $\Delta\psi_{ij}$ is the constant difference in phase between nodes i and j.

To illustrate the notion of delayed equivalence, see, for example, the setup described in Fig. 1. The structure is composed of 11 "cells" having the same configuration and two additional cells with a mirror-reflected configuration. The structure spins with constant angular velocity ω around the z axis and is exposed to constant one-directional solar radiation. The truss is assumed to be covered with an opaque material (which does not play any thermal role). Thus, one-half of the structure is always overshadowed by the other half. Suppose for simplicity that each truss member is represented by one finite element. Overall there are 52 joints, which are also finite element nodes. These nodes can be divided into 19 equivalence groups. The first group includes the four right-most nodes, numbered 1-4. The graphs that describe the temperature variation of these four nodes will be identical up to a rigid shift in time: nodes 2, 3, and 4 will have the same temperature as node 1, with phase differences of 90, 270, and 180 deg, respectively. These are altogether seven groups of four nodes; each has the same pattern. In addition, there are 12 groups of two nodes each, with a phase difference of 180 deg between each two nodes. The first four of these groups are (29,36); (30,35); (31,34); and (32,33). Thus, every one of the 52 nodes belongs to one of the 19 equivalence groups. One of the nodes in each of these groups is chosen (arbitrarily) as the *representative node* of its group, and all of the nodes in the same group can be thought of as shifted in phase with respect to the node.

It is easy to see that this type of symmetry may be exploited in the present method, since phase shift constants are simply translated into multiplying factors in the final system of equations [e.g., $\sin n(\psi + \Delta\psi_{ij}) = (\cos n\Delta\psi_{ij})\ \sin n\psi + (\sin n\Delta\psi_{ij})\ \cos n\psi$]. All of the unknowns associated with a certain node can be expressed in terms of the corresponding unknowns associated with the representative node of the same group. Doing this may lead to a significant reduction in computational cost and in required storage. For example, instead of the original $52(2N + 1)$ unknowns in the problem described in Fig. 1, we are left with only $19(2N + 1)$ unknowns. It is important to note that the solution method used here, which incorporates Fourier decomposition in time, is especially appropriate for taking advantage of this type of symmetry, while other methods, such as implicit time-integration, are not capable of treating such symmetry with comparable simplicity.

A similar technique can be applied in the elastic analysis. One should note, however, that, in the elastic case, the degrees of freedom, not the nodes, have phase shift relations between them. These relations involve vector transformation between the displacements in the fixed global coordinate system and the displacements expressed in a local coordinate system rotating with the structure.

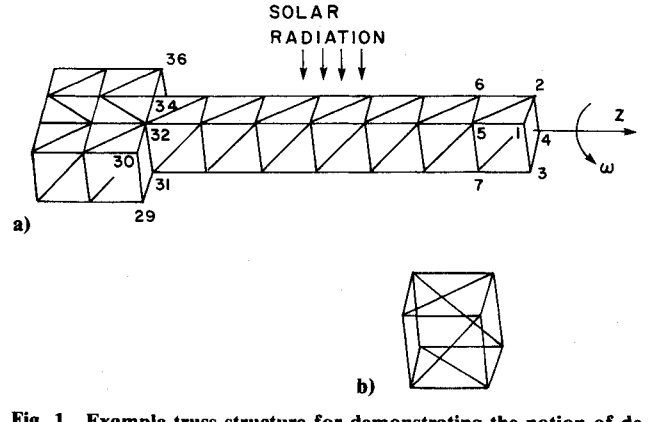

Fig. 1 Example truss structure for demonstrating the notion of delayed equivalence; also shown is a typical cell composing the structure.

Finding the External Heat Flux Distribution

Whether the space structure rotates around a certain axis or orbits around the Earth, the orientation of each truss member changes in time with respect to the direction of the incoming solar heat flux vector q_{sun}. Other external sources of heat flux are Earth-emitted and Earth-reflected radiation, but for simplicity only solar radiation will be considered here. Let $q_{sun} = q_{sun}b$, where q_{sun} is the magnitude of the solar radiation and b is a fixed unit vector indicating its direction. If q_i denotes the external normal heat flux that member i absorbs, then generally

$$q_i(t) = \alpha_s \frac{p}{A} \beta_i(t) q_{sun} \tag{7}$$

where α_s is the surface absorptivity, p/A is the same as in Eq. (3), and β_i is the so-called view factor associated with member i (and with the sun).

Considering the structure in Fig. 1 again, there are four types of truss members in this model: members that are parallel to the axis of rotation z (such as the member joining nodes 3 and 7), members that are vertical to z (such as the member 1-2), diagonal members (such as 1-7), and internal members that are never exposed to solar radiation (there are six of those). Figure 2 shows the view factor β_i as a function of the azimuth angle for the first three types of members (β_i for the fourth type is identically zero). The graph of β_i for a "vertical member" is that of a truncated sine, the one for a "parallel member" has a step-function character, and the graph for a diagonal member lies between the former two. There is, of course, a phase-angle shift between the view factors of two truss members of the same type.

For a large and complicated space structure, the calculation of the view factor $\beta_i(t)$ for each truss member is best done automatically as a preprocess before the analysis. The following algorithm performs this calculation for a general rotating space structure. Each truss member may belong either to a transparent part or to an opaque part of the structure, and the member can be either external or internal. This algorithm is an adaptation of the common "projected-area" algorithm for the general opaque/transparent time-dependent problem.

It is assumed that the coordinates of the joints are given in a fixed reference Cartesian system (X, Y, Z), where Z is the axis of rotation, and that there are a total number of N_{tm} members in the truss.

The algorithm can be outlined as follows. Each truss member is treated separately in the manner to be described, except for internal members belonging to an opaque part of the structure, which are given a zero view factor from the outset.

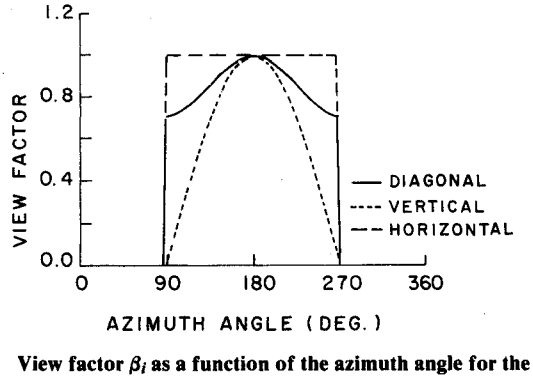

Fig. 2 View factor β_i as a function of the azimuth angle for the three types of truss members in the structure of Fig. 1.

Let i be the current truss member under consideration, and let j indicate one of its two joints. Then for $j=1, 2$, the radial distance of joint j from the axis of rotation R_j and the reference angle of joint j, Φ_j are calculated. This enables one to obtain the instantaneous coordinates of joint j, denoted $x_j(t)$, $y_j(t)$, and z_j. The next step is to calculate $\boldsymbol{r}(t)$, the horizontal radial vector pointing to the center of the member, and $\boldsymbol{s}(t)$, a vector tangent to the member. Next, the plane P: $Ax+By+Cz=0$, which is the instantaneous plane containing the member and the solar radiation vector, is defined by determining the parameters $A(t)$, $B(t)$, and $C(t)$. Then we calculate $\boldsymbol{n}(t)$, a vector lying on plane P and normal to the member, and $\boldsymbol{e}(t)$, the unit vector lying on plane P, normal to the member and pointing in the outward direction. Finally, the view factor $\beta_i(t)$ is found. It depends on the vectors $\boldsymbol{b}$ and $\boldsymbol{e}(t)$ and on whether member i belongs to a transparent or to an opaque part of the structure.

Algorithm for Computing View Factors for a General Rotating Space Structure

1) Given: the solar radiation vector $\boldsymbol{q}_{\text{sun}}=q_{\text{sun}}\boldsymbol{b}$, the angular velocity ω, the reference coordinates of all the joints, set $i=0$.

2) Advance the member number $i \leftarrow i+1$. If $i>N_{tm}$, stop.

3) Determine the reference coordinates of the two joints of member i: (X_1, Y_1, Z_1) and (X_2, Y_2, Z_2). Determine also whether member i belongs to an opaque part or to a transparent part of the structure and whether the member is external or internal.

4) If member i belongs to an opaque part of the structure *and* it is internal, set $\beta_i=0$, and go back to step 2.

5) For $j=1, 2$, calculate

$$R_j=\sqrt{X_j^2+Y_j^2}; \qquad \Phi_i=\arctan Y_j/X_j$$

$$x_j(t)=R_j\cos(\omega t+\Phi_j); \quad y_j(t)=R_j\sin(\omega t+\Phi_j); \quad z_j=Z_j$$

6) Calculate

$$\boldsymbol{r}(t)=[x_1(t)+x_2(t),\ y_1(t)+y_2(t),\ 0]$$

$$\boldsymbol{s}(t)=[x_2(t)-x_1(t),\ y_2(t)-y_1(t),\ z_2-z_1]$$

$$A(t)=s_2(t)b_3-s_3b_2$$

$$B(t)=s_3b_1-s_1(t)b_3$$

$$C(t)=s_1(t)b_2-s_2(t)b_1$$

$$\boldsymbol{n}(t)=[-C(t)s_2(t)+B(t)s_3,\ -A(t)s_3+C(t)s_1(t),$$
$$-B(t)s_1(t)+A(t)s_2(t)]$$

$$\boldsymbol{e}(t)=\boldsymbol{n}(t)/|\boldsymbol{n}(t)|\ \text{sign}\ [\boldsymbol{r}(t)\cdot\boldsymbol{n}(t)]$$

$$\lambda(t)=\boldsymbol{b}\cdot\boldsymbol{e}(t)$$

7) If member i belongs to a transparent part of the structure, then

$$B_i(t)=|\lambda(t)|$$

Otherwise,

$$\beta_i(t)=\begin{cases}|\lambda(t)|; & \text{if } \lambda(t)<0\\ 0; & \text{if } \lambda(t)\geq 0\end{cases}$$

8) Next i (go back to step 2).

The algorithm given above together with Eq. (7) determines the function $q_i(t)$, i.e., the external thermal loading on each truss member. This function is incorporated in an FFT routine for the calculation of the Fourier coefficients Q_0, Q_{cn}, *and* Q_{sn}, for $n=1, \ldots, N$, as mentioned in the previous section.

Numerical Results and Discussion

Two models are now analyzed using the numerical method described in the previous sections. The first model is that of a cylindrically shaped space structure made of a composite graphite-epoxy material and spinning around its axis. The structure is shown in Fig. 3. The two ends of the cylinder are assumed to be fixed to rigid bases, so that they are constrained to rotate without deformation. The thermal and mechanical properties of graphite-epoxy are $\rho c=1.76\times10^6$ J/m^3 K, $k=10.1$ W/m K, $C_R=9.1\times10^{-7}$ W/m^3 K^4, $\alpha_s=0.92$, $\rho A=51.3$ kg/m, $EA=1.41\times10^6$ N, $\alpha=7.3\times10^{-7}$ 1/K. Other parameters are $q_{\text{sun}}=1300$ W/m^2, $T_{\text{ref}}=299$ K, and $p/A=20$ m^{-1}. The cylinder is length 6 m and radius 1.4 m. Each truss member is represented by one finite element with linear shape functions.

The thermal analysis is considered first. Although the structure contains 50 joints, the temperatures at only three of them are independent unknowns, since the rest of the nodes are equivalent to one of these three in the sense of delayed equivalence explained before. In the present model, nodes 1, 2, and 3 in Fig. 3 were chosen as representative nodes.

The structure is first assumed to be covered with an opaque material, so self-shadowing effects are present. The angular speed is set to $\omega=10^{-5}$ rad/s, namely the structure rotates very slowly. As a preceding step, in order to determine the minimal number of harmonics needed in the temporal Fourier decomposition, the analysis was performed repeatedly with a different number of harmonics. In Fig. 4, the temperature at repre-

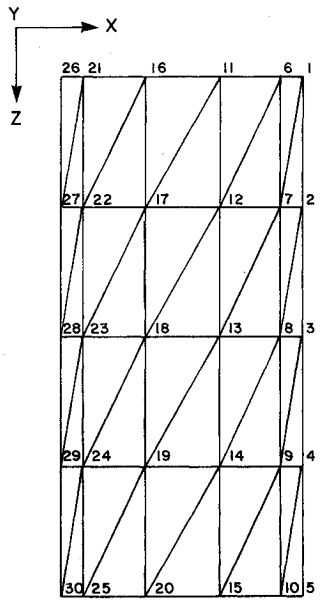

Fig. 3 Cylindrically shaped truss model. Each truss member is represented by a single finite element.

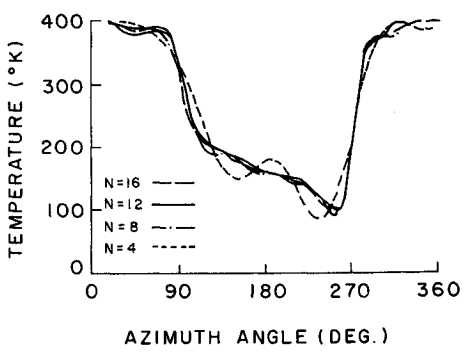

Fig. 4 Temperature variation at representative node number 1 of the cylindrical structure, with $\omega=10^{-5}$ rad/s and using 4, 8, 12, and 16 harmonics.

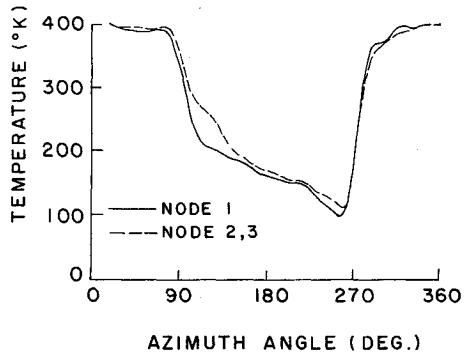

Fig. 5 Temperature variation at the three representative nodes of the cylindrical structure, with $\omega = 10^{-5}$ rad/s.

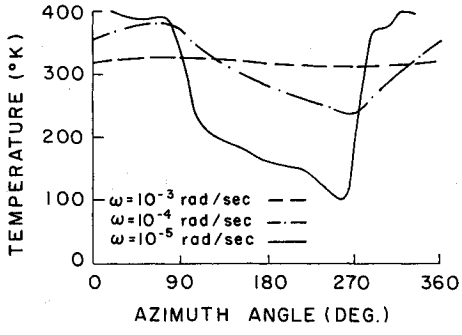

Fig. 6 Temperature variation at representative node number 1 of the cylindrical structure, with $\omega = 10^{-5}$ rad/s, $\omega = 10^{-4}$ rad/s, and $\omega = 10^{-3}$ rad/s.

sentative node 1 as a function of the azimuth angle (or time) is shown, for the cases where 4, 8, 12, and 16 harmonics were used. It is apparent from the graphs that convergence is practically achieved with 12 harmonics and, that for a smaller number of harmonics, the solution obtained is quite inaccurate. For this reason, all of the numerical simulations described below have been performed with 12 harmonics.

In Fig. 5 the solution at the three representative nodes is shown. The temperature in the unshaded region is 400 K; whereas it reaches a minimum value of about 100 K in the shaded region. Thus, with an angular velocity of $\omega = 10^{-5}$ rad/s, the temperature is undergoing large variations in time and in the spatial circumferential direction. On the other hand, it is clear that the variation of temperature along the axial direction z (which manifests itself in the difference between the temperatures at nodes 1, 2, and 3) is small.

The thermal analysis is now repeated with higher and lower values of ω. It turns out that the temperature distribution of Fig. 5 remains unchanged when ω is decreased, and in fact the same solution is practically obtained for the quasisteady state $\omega = 0$. On the other hand increasing ω above the value of 10^{-5} rad/s makes the variations in the temperature field smaller. This can be seen in Fig. 6 where the solutions corresponding to angular speeds of $\omega = 10^{-5}$ rad/s, $\omega = 10^{-4}$ rad/s, and $\omega = 10^{-3}$ rad/s are shown. For the case $\omega = 10^{-3}$, the temperature is almost constant (330 K). This can be regarded as the "fully-dynamic" state; the structure spins so fast that no significant temperature differences develop between the shaded and unshaded regions.

These numerical results show that the transition from the quasisteady state to a fully-dynamic state occurs around $\omega = 10^{-4}$ rad/s. The small value of this angular velocity means that special care must be taken when making the assumption of a quasisteady motion, because even for a very slowly rotating structure this assumption might be inappropriate.

A rough estimate for the transitional angular speed can be obtained *analytically* from the following simple model problem. Consider a fixed straight rod of length L, which is exposed to incoming heat flux given by $q(t) = q_0 \sin\omega t$, and suppose that the temperature at the two ends is kept 0 at all times. Note that the same heat flux variation is imposed if $q = q_0$ and the rod is *rotating* with angular speed ω, which is the situation with which we are actually interested. In order to be able to treat the problem analytically, the radiation emitted by the rod is neglected here. Of course, the simplifying assumptions made here are too drastic to give accurate information with respect to a specific space structure configuration. The goal is merely to obtain the order of magnitude of the transitional angular speed.

The mathematical problem is to find a time-periodic solution $T(x,t)$, which satisfies the equations

$$\rho c\dot{T} = kT'' + q_0 \sin\omega t \tag{8}$$

$$T(0,t) = T(L,t) = 0 \tag{9}$$

A quasisteady assumption is justified if

$$|\rho c\dot{T}| \ll |q_0 \sin\omega t| \tag{10}$$

for any x and any t. When this is the case, one may omit the term $\rho c\dot{T}$ from Eq. (8). Then the solution of Eqs. (8) and (9) is simply

$$T_{QS} = \frac{q_0}{2k}(L - x)x \sin\omega t \tag{11}$$

Now the consistency of the quasisteady solution of Eq. (11) can be checked against the original quasisteady assumption. In order to do this, we consider a weakened version of Eq. (10), where only the *averages* in time and space of the quantities appearing in Eq. (10) are required to satisfy the inequality. In other words, we replaced Eq. (10) by

$$\frac{1}{2\pi L}\int_0^L \int_0^{2\pi} |\rho c\dot{T}_{QS}| \mathrm{d}\phi \mathrm{d}x \ll \frac{1}{2\pi L}\int_0^L \int_0^{2\pi} |q_0 \sin\phi| \mathrm{d}\phi \mathrm{d}x \tag{12}$$

Using the quasisteady solution of Eq. (11) in Eq. (12) yields after simple algebra the requirement

$$\omega \ll \frac{12k}{\rho c L^2} \tag{13}$$

Substituting the numerical values of k and ρc for graphite-epoxy in Eq. (13) and using a typical length of $L = 1$ m, one obtains the (necessary) condition $\omega_{QS} \ll 7 \times 10^{-5}$ rad/s for the validity of the quasisteady assumption. This value agrees with our previous numerical results. Thus, the angular speed corresponding to the transition between steady state and fully-dynamic state can be estimated quite well with the simple analytic calculation performed here. We remark that angular speeds of order 10^{-5} rad/s are typical for a geosynchronous orbiting spacecraft, as will be seen in the second model to be considered.

The thermal analysis is performed now again, but this time the structure is assumed to be totally transparent. The angular speed is set to $\omega = 10^{-5}$ rad/s. Figure 7 describes the temperature at the three representative nodes as a function of the azimuth angle. As expected, the temperature field is much more uniform in comparison to the field generated with the same angular speed in the opaque case (see, for example, Fig. 5).

Now we turn to the thermoelastic analysis of the structure, based on the temperature field just found. The delayed equivalence symmetry is exploited here as well. Since there are three

degrees of freedom per node and due to the prescribed boundary conditions, there are nine equivalence groups (excluding the group of degrees of freedom on the fixed boundary). Using 12 harmonics in the Fourier decomposition, this means that there only 225 unknowns out of the 2250 unknowns that one would have if advantage were not taken of symmetry. This obviously leads to great saving in computational effort and storage requirements.

We consider the case where the structure is opaque and rotating with $\omega = 10^{-5}$ rad/s. Figure 8 shows the deformed mesh at time $t = 0$ (which is identical to the deformation at times $t = 2\pi/\omega$, $t = 4\pi/\omega$, etc., due to the periodicity of the motion). The displacements are magnified by a factor of 200. The self-shadowing effect is apparent in the figure: the part of the structure exposed to solar radiation at time $t = 0$ expands much more than the shaded part of the structure, which gives rise to the unsymmetrical deformation observed.

The elastic analysis was repeated while neglecting the inertial term $\rho A\ddot{u}$ in Eq. (2). This produced practically the same results as before, which implies that the elastic problem can be regarded as quasisteady. The same was found to be true for much higher angular speeds. Again this fact can be demonstrated via a simple analytical model, as was done in the thermal case. Solving the quasisteady version of the problem

$$\rho A\ddot{u} = EAu'' + f_0 \sin\omega t \tag{14}$$

$$u(0,t) = u(L,t) = 0 \tag{15}$$

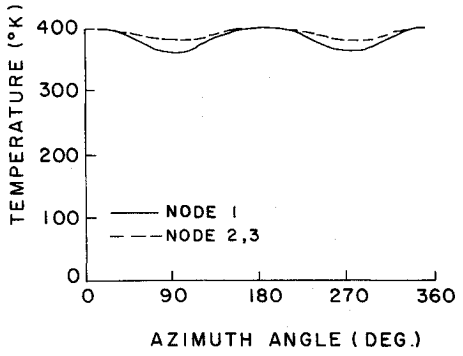

Fig. 7 Temperature variation at the three representative nodes of the cylindrical structure, with $\omega = 10^{-5}$ rad/s and assuming total transparency.

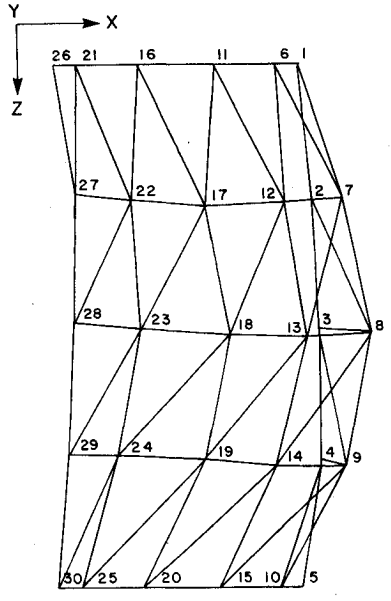

Fig. 8 Deformed cylindrical structure at time $t = 0$, with the displacements magnified by a factor of 200.

and requiring weak consistency [see, for example, Eqs. (8) – (13)], yields the condition

$$\omega \ll \sqrt{\frac{12E}{\rho L^2}} \tag{16}$$

Substituting the numerical values corresponding to graphite-epoxy and using $L = 1$ m, one obtains $\omega_{QS} \ll 1.8 \times 10^4$ rad/s. Thus, the typical angular speed at the transition between the quasisteady and fully-dynamic cases is about 8 order of magnitudes larger than the one obtained in the thermal analysis. Therefore, for all practical angular speeds, the motion can always be regarded as quasisteady as far as the elastic analysis is concerned.

We turn now to the analysis of a parabolic antenna dish mounted on a spacecraft, which orbits around the Earth, as illustrated in Fig. 9. The orientation of the antenna changes (with respect to the solar radiation vector) such that it always faces the Earth. For simplicity we assume that during one-half of the period the structure is totally exposed to solar radiation; whereas during the other half of the period it is hidden from the sun by the Earth. Figure 10 describes the geometry of the antenna considered. The inner circular loop of radius 5 m is fixed to a rigid frame. The outer circular loop is of radius 20 m, and the depth of the parabolic dish is 6 m. The material properties are the same as in the previous structure. It is assumed that the spacecraft is geosynchronous, i.e., it completes one period around the Earth in 24 h. In other words, $\omega = 7.27 \times 10^{-5}$ rad/s, which is in the transition region between quasisteady and fully-dynamic motions.

There are 15 symmetry equivalence groups in the thermal analysis, and we again use 12 harmonics throughout the calculation. The representative nodes are numbered 1–15 in Fig. 10.

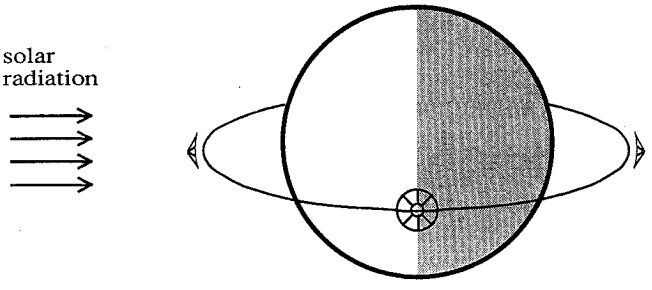

Fig. 9 Parabolic antenna dish mounted on a spacecraft which orbits around the Earth; the orientation of the various members with respect to the sun changes during the motion.

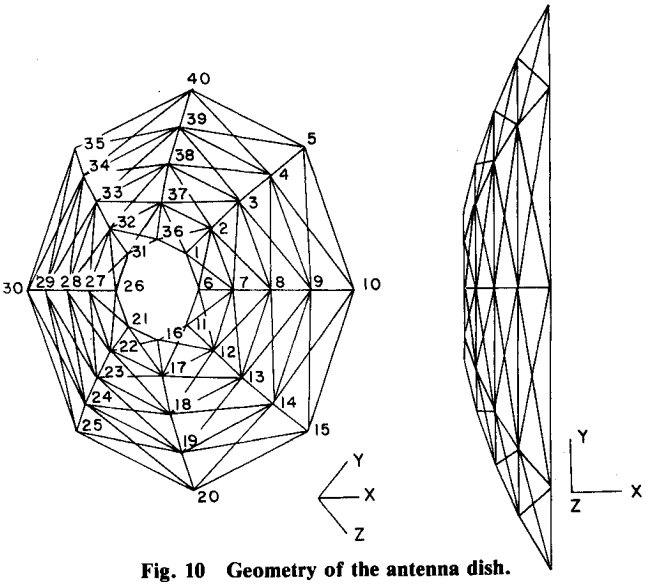

Fig. 10 Geometry of the antenna dish.

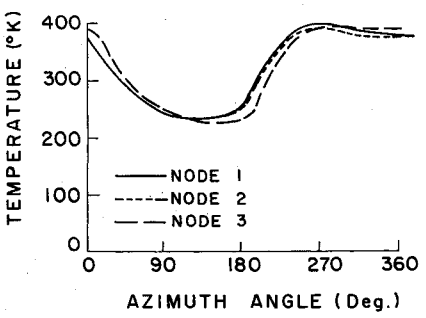

Fig. 11 Temperature variation at the representative nodes 1, 2, and 3 of the antenna dish.

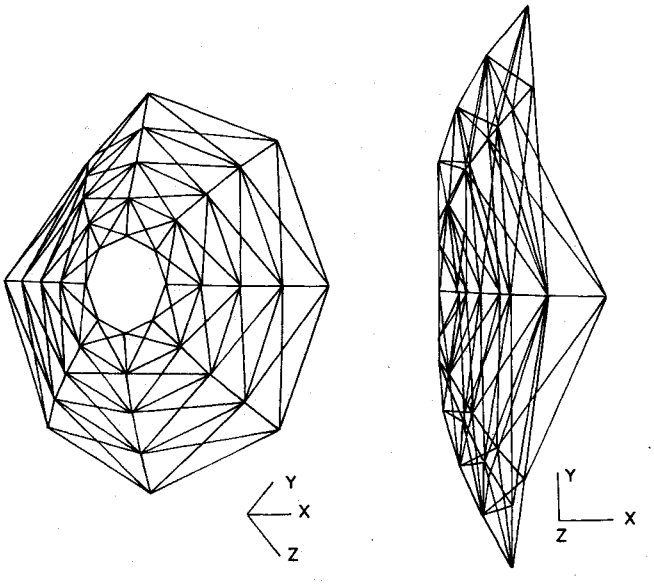

Fig. 12 Deformed antenna structure at time $t = 0$, with the displacements magnified by a factor of 500.

In Fig. 11 the temperature variation in the representative nodes 1, 2, and 3 during one period is plotted. Again, large variations in time are apparent: the temperature varies between 230 and 400 K.

In the elastic analysis, there are 36 equivalence groups and a total of 900 unknowns. Figure 12 illustrates the deformed structure at time $t = 0$, i.e., when the back side of the dish faces the sun symmetrically. A scaling factor of 500 is used to magnify the deformation. The asymmetry present in the figure is typical to the angular speed in which the dish rotates, which is the transitional speed between the quasisteady state and the fully-dynamic state. In much higher or much lower angular speeds, the deformation tends to be symmetric.

Although it was established that the proposed methodology is effective in solving thermal and thermoelastic problems of space structures, the analysis performed here was restricted under the quite severe list of assumptions outlined previously. In particular, assumptions 2 and 6 in that list are in many practical cases far from being true. Joints are not perfect conductors due to the imperfect mating of the surface, and their mass is quite significant to the overall problem. Also, assumption 1 may be unjustified in some cases. Not using this assumption makes the thermal problem a three-dimensional one and adds bending as a mode of deformation of the truss members. Therefore, analysis of practical engineering problems using the proposed method still awaits improvements.

Concluding Remarks

A new method has been proposed for the thermal and thermoelastic analysis of large truss-type space structures undergoing periodic motion. Symmetry with respect to the axis of rotation is fully exploited, which may lead to considerable saving in computing time and storage requirements. The method has been employed to solve two typical, although somewhat simplified, problems of large space structures.

As far as the characterization of a given problem as quasisteady, fully dynamic, or transitional is concerned, the implication of the analysis is that while the elastic response can be regarded as quasisteady for all practical motions, special care must be taken when considering the thermal problem. Even for a very slowly rotating structure, the thermal steady state assumption might be inappropriate. In such cases, a rough estimate of the critical angular speed may be obtained from the analytic analysis of a much simplified one-dimensional model problem. Small angular speeds, for which the structure may be in the transitional region between a quasisteady and a fully dynamic response, are typical, for example, for satellites in geosynchronous orbit.

The proposed method seems to constitute an attractive approach for the analysis of time-periodic space structures. Notwithstanding, the analysis performed in this paper is based on some restrictive assumptions that need to be relaxed in various combinations in future investigations. In particular, three-dimensional effects resulting from the variation of temperature in the cross section of the members should be included.

Acknowledgments

We wish to thank the reviewers for their helpful remarks. This work was supported in part by the L. Kraus Research Fund, Vice President Research Fund 160-613.

References

[1]Foldes, P., and Dienemann, M. W., "Large Multibeam Antennas for Space," *Journal of Spacecraft and Rockets*, Vol. 17, July-Aug. 1980, pp. 363-371.

[2]Archer, J. S., "High Performance Parabolic Antenna Reflectors," *Journal of Spacecraft and Rockets*, Vol. 17, Jan.-Feb. 1980, pp. 20-26.

[3]Clark, S. C., and Allen, G. E., "Thermo-Mechanical Design and Analysis System for the Hughes 76-in. Parabolic Antenna Reflector," *Spacecraft Thermal Control, Design, and Operation*, edited by H. E., Collicott and P. E. Bauer, AIAA, New York, 1983, pp. 109-129.

[4]Mikulas, M. M., Croomes, S. D., Schneider, W., Bush, H. G., Nagy, K., Pelischek, T., Lake, M. S., and Wesselski, C., "Space Station Truss Structures and Construction Considerations," NASA TR-86338, 1985.

[5]Nash, W. A., and Lardner, T. J., "Parametric Investigation of Factors Influencing the Mechanical Behavior of Large Space Structures," Air Force Office of Scientific Research, Rept. TR-86-0858, 1985.

[6]Anderson, M. S., and Nimmo, N. A., "Determinate Space-Truss Platforms," *Proceedings of the 26th Structures, Structural Dynamics and Materials Conference*, Pt. 2, AIAA, New York, 1985, pp. 723-728.

[7]Ard, K. E., "Design and Technology Study for Extreme Precision Antenna Structures," NASA CR-174861, 1985.

[8]Hedgepeth, J. M., and Miller, R. K., "Structural Concepts for Large Solar Concentrators," *Acta Astronautica*, Vol. 17, Jan. 1988, pp. 79-89.

[9]Peskett, S. C., and Gethin, D. T., "Thermal Analysis of Spacecraft," *Numerical Methods in Thermal Problems*, Vol. VI, Pt. 1, edited by R. W. Lewis and K. Morgan, Pineridge Press, Swansea, England, UK, 1989, pp. 713-729.

[10]Ory, H., Menking, M., Hornung, E., and Erben, E., "Development of Large Orbital Structure Systems," 40th Congress of the IAF, Beijing, China, Paper IAF-89-340, International Astronautical Federation, 1989.

[11]Thornton, E. A., Dechaumphai, P., and Wieting, A. R., "Integrated Finite Element Thermal-Structural Analysis with Radiation Heat Transfer," *Proceedings of the 23rd Structures, Structural Dynamics and Materials Conf.*, Pt. 1, AIAA, New York, 1982, pp. 188-196.

[12]Thornton, E. A., and Paul, D. B., "Thermal-Structural Analysis of Large Space Structures: An Assessment of Recent Advances," *Journal of Spacecraft and Rockets*, Vol. 22, July-Aug. 1985, pp. 385-393.

[13]Mahaney, J., and Thornton, E. A., "Self-Shadowing Effects on the Thermal-Structural Response of Orbiting Trusses," *Journal of Spacecraft and Rockets*, Vol. 24, July-Aug. 1987, pp. 342–348.

[14]Ko, W. L., "Solution Accuracies of Finite Element Reentry Heat Transfer and Thermal Stress Analyses of Space Shuttle Orbiter," *International Journal of Numerical Methods Engineering*, Vol. 25, No. 2, 1988, pp. 517–543.

[15]Lutz, J. D., Allen, D. H., and Haisler, W. E., "Finite-Element Model for the Thermoelastic Analysis of Large Composite Space Structures," *Journal of Spacecraft and Rockets*, Vol. 24, Sept.–Oct. 1987, pp. 430–436.

[16]Rand, O., and Givoli, D., "A Finite Element Spectral Method With Application to the Thermoelastic Analysis of Structures," *Journal of Numerical Methods Engineering,* Vol. 30, Aug. 1990, pp. 291–306.

[17]Rand, O., "Harmonic Variables—A New Approach to Nonlinear Periodic Problems," *Journal of Computers and Mathematics with Applications,* Vol. 15, No. 11, 1988, pp. 953–961.

Earl A. Thornton
Associate Editor